Prostaglandin E2 is essential for efficacious skeletal muscle stem-cell function, augmenting regeneration and strength

Andrew T. V. Ho[a,1], Adelaida R. Palla[a,1], Matthew R. Blake[a], Nora D. Yucel[a], Yu Xin Wang[a], Klas E. G. Magnusson[a,b], Colin A. Holbrook[a], Peggy E. Kraft[a], Scott L. Delp[c], and Helen M. Blau[a,2]

[a]Baxter Laboratory for Stem Cell Biology, Department of Microbiology and Immunology, Institute for Stem Cell Biology and Regenerative Medicine, Stanford School of Medicine, Stanford, CA 94305-5175; [b]Department of Signal Processing, Autonomic Complex Communication Networks, Signals and Systems Linnaeus Centre, Kungliga Tekniska Högskolan Royal Institute of Technology, 100 44 Stockholm, Sweden; and [c]Department of Bioengineering, Stanford University School of Medicine, Stanford, CA 94305

This contribution is part of the special series of Inaugural Articles by members of the National Academy of Sciences elected in 2016.

Contributed by Helen M. Blau, May 15, 2017 (sent for review April 3, 2017; reviewed by Douglas P. Millay and Fabio M. V. Rossi)

Skeletal muscles harbor quiescent muscle-specific stem cells (MuSCs) capable of tissue regeneration throughout life. Muscle injury precipitates a complex inflammatory response in which a multiplicity of cell types, cytokines, and growth factors participate. Here we show that Prostaglandin E2 (PGE2) is an inflammatory cytokine that directly targets MuSCs via the EP4 receptor, leading to MuSC expansion. An acute treatment with PGE2 suffices to robustly augment muscle regeneration by either endogenous or transplanted MuSCs. Loss of PGE2 signaling by specific genetic ablation of the EP4 receptor in MuSCs impairs regeneration, leading to decreased muscle force. Inhibition of PGE2 production through nonsteroidal anti-inflammatory drug (NSAID) administration just after injury similarly hinders regeneration and compromises muscle strength. Mechanistically, the PGE2 EP4 interaction causes MuSC expansion by triggering a cAMP/phosphoCREB pathway that activates the proliferation-inducing transcription factor, *Nurr1*. Our findings reveal that loss of PGE2 signaling to MuSCs during recovery from injury impedes muscle repair and strength. Through such gain- or loss-of-function experiments, we found that PGE2 signaling acts as a rheostat for muscle stem-cell function. Decreased PGE2 signaling due to NSAIDs or increased PGE2 due to exogenous delivery dictates MuSC function, which determines the outcome of regeneration. The markedly enhanced and accelerated repair of damaged muscles following intramuscular delivery of PGE2 suggests a previously unrecognized indication for this therapeutic agent.

muscle stem cells | PGE2 | regeneration | NSAIDs | strength

Satellite cells, also known as muscle stem cells (MuSCs), are crucial to muscle regeneration. They reside in a quiescent state in niches juxtaposed to myofibers in muscle tissues, poised to respond to damage and repair skeletal muscles throughout life (1–4). Muscle injury precipitates an inflammatory response that is marked by the sequential infiltration of multiple cell types, including neutrophils, monocytes, macrophages, T cells, and fibroadipocytes, and is accompanied by MuSC activation. During this inflammatory phase, concurrent waves of cytokines and growth factors are released, including CC-chemokine ligand 2 (CCL2), IL-10, IL-1β, tumor necrosis factor-α (TNFα), and transforming growth factor-β1 (TGFβ1) (3, 5–10). In addition, prostaglandins, potent lipid mediators of inflammation, are synthesized and secreted by immune and myogenic cells (6, 11). Prostaglandins derive from arachidonic acid, which is released from membrane phospholipids by phospholipase A2 and converted by cyclooxygenase enzymes (COX-1 and -2) into prostaglandin H2 (PGH2) and subsequently into the different prostaglandin subtypes, PGD2, PGE2, PGF2α, PGI2, or thromboxane (TXA2). Specific to the generation of PGE2 are the prostaglandin synthases (PGES: mPGES-1, mPGES-2, and cPGES) (11–13).

PGE2 has been associated with muscle regeneration, however its specific mode of action remains unclear. Conflicting reports suggest that PGE2 can either promote myoblast proliferation or differentiation in culture (14–18). In the COX-2–knockout mouse model, which lacks PGE2, regeneration is delayed. However, the mechanism by which PGE2 acts could not be established in these studies due to the systemic constitutive loss of COX-2 and consequent nonspecific effects on many cell types (15, 19). Similarly, muscle recovery after injury was impaired in mice given a COX-2 inhibitor (15). Additionally, mice treated with nonsteroidal anti-inflammatory drugs (NSAIDs), which block the production of prostaglandins through inhibition of COX-1 and COX-2, exhibited regeneration deficits (20, 21). Moreover, NSAIDS lead to an attenuation of exercise-induced expansion of human satellite cells in biopsies (20). Likewise, glucocorticoids, which reduce prostaglandin synthesis by suppressing phospholipase A2, COX-2, and mPGES1 expression, adversely affect the recovery of muscle strength in polymyositis patients (22). However, because the target of NSAIDs and glucocorticoids are the COX enzymes, this effect could entail a number of prostaglandin subtypes

Significance

Muscle repair after injury entails an immune response that orchestrates efficacious regeneration. Here we identify Prostaglandin E2 (PGE2) as a crucial inflammatory mediator of muscle stem cells (MuSCs), the building blocks of muscle regeneration. PGE2 is synthesized and secreted into the stem-cell niche in response to injury, leading to robust MuSC proliferation, key to myofiber repair. EP4 is the receptor that mediates PGE2 signaling in MuSCs, and genetically engineered mice that lack EP4 in MuSCs have impaired regeneration. Nonsteroidal anti-inflammatory drugs (NSAIDs), commonly used to treat pain after muscle injury, inhibit PGE2 synthesis, hinder muscle regeneration, and lead to weakened muscles. Importantly, a single treatment of injured muscles with PGE2 dramatically accelerates muscle repair and recovery of strength.

Author contributions: A.T.V.H., A.R.P., S.L.D., and H.M.B. designed research; A.T.V.H., A.R.P., M.R.B., N.D.Y., Y.X.W., C.A.H., and P.E.K. performed research; A.T.V.H., A.R.P., M.R.B., N.D.Y., K.E.G.M., C.A.H., and H.M.B. analyzed data; and A.T.V.H., A.R.P., and H.M.B. wrote the paper.

Reviewers: D.P.M., Cincinnati Children's Hospital Medical Center; and F.M.V.R., The Biomedical Research Center.

Conflict of interest statement: A.T.V.H., A.R.P., and H.M.B. are named inventors on a patent related to the findings in this paper. H.M.B. and S.L.D. are cofounders of the company Myoforte.

Freely available online through the PNAS open access option.

Data deposition: The data reported in this paper have been deposited in the Gene Expression Omnibus (GEO) database, https://www.ncbi.nlm.nih.gov/geo (accession no. GSE97375).

[1]A.T.V.H. and A.R.P. contributed equally to this work.

[2]To whom correspondence should be addressed. Email: hblau@stanford.edu.

This article contains supporting information online at www.pnas.org/lookup/suppl/doi:10.1073/pnas.1705420114/-/DCSupplemental.

in addition to PGE2 and therefore have pleiotropic effects. Thus, to date, the spatiotemporal effects of PGE2 in muscle regeneration remain unresolved.

In response to injury, PGE2 is transiently induced in muscle tissues. To establish if PGE2 acts directly on MuSCs, the building blocks of muscle regeneration, we generated mice in which the PGE2 receptor, EP4, could be conditionally ablated in MuSCs. In addition, we established transgenic reporter mice that enabled specific tracking of MuSC contribution to regeneration dynamically and sensitively over time by bioluminescence imaging (BLI) after PGE2 delivery. We coupled these models with assays of muscle force and found a direct link between the ability of MuSCs to respond to PGE2 and regeneration, leading to restoration of force. Gain- and loss-of-function experiments revealed that PGE2 signaling acts as a rheostat for MuSC function. Our data suggest that PGE2 profoundly impacts regeneration and has therapeutic promise.

Results

A Surge of PGE2 in Damaged Muscle Tissues Accelerates MuSC Proliferation. We sought to identify an activator of MuSC function by capitalizing on an inflammatory response that mediates muscle regeneration. Because muscle injury triggers an immediate inflammatory response (5, 7, 8, 23), we hypothesized that a transiently induced inflammatory modulator could regulate MuSC function and play a crucial role in regeneration. We performed qRT-PCR and detected increased levels of the *Ptger4* receptor (EP4) for

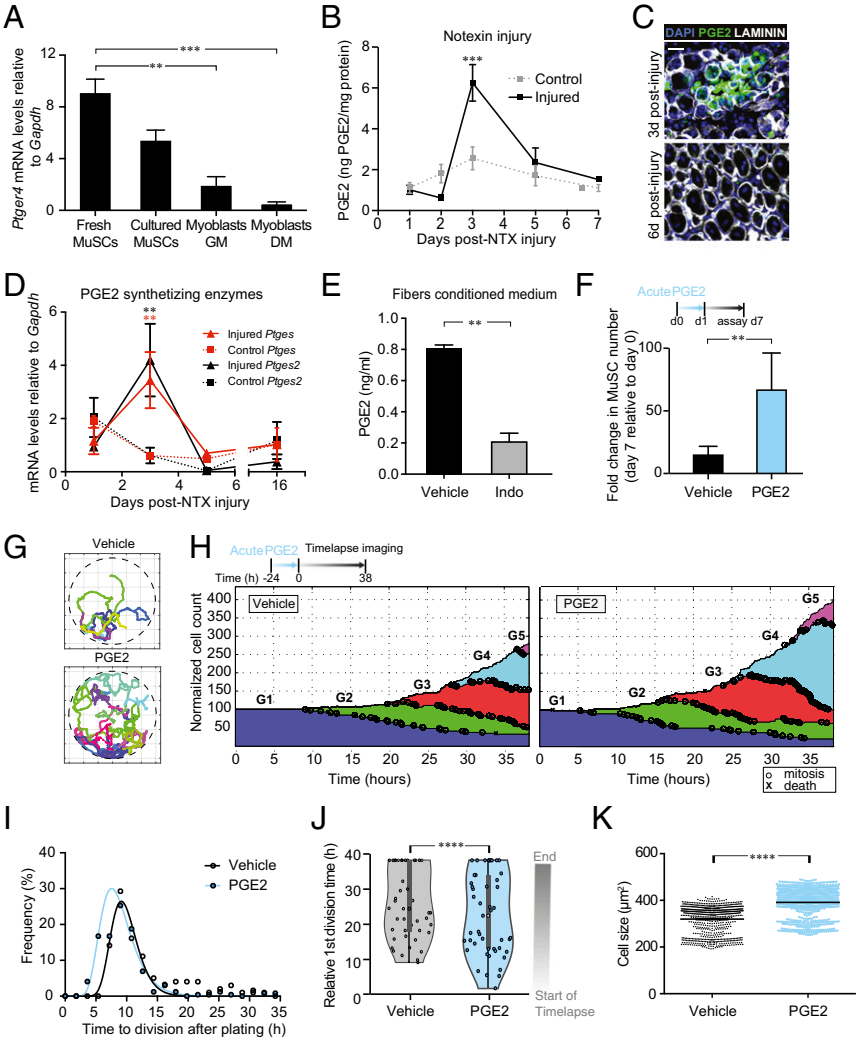

Fig. 1. Transient increase in PGE2 in damaged muscle tissues accelerates MuSC proliferation. (*A*) Expression of *Ptger4* in freshly isolated MuSCs from uninjured mouse hindlimbs (Fresh MuSCs), MuSCs cultured for 2 d on hydrogels (Cultured MuSCs), primary myoblasts cultured in growth medium (Myoblasts GM), and differentiating primary myoblasts cultured in differentiation medium for 24 h (Myoblasts DM) ($n = 3$ biological replicates per condition). (*B*) PGE2 levels assayed by ELISA after tibialis anterior (TA) muscle injury with notexin ($n = 4$ mice per condition measured). Control refers to the contralateral uninjured leg. (*C*) Representative TA cross-sections of 3 and 6 d after notexin injury. DAPI, blue; LAMININ, white; PGE2, green. (Scale bar, 40 µm.) (*D*) Expression of prostaglandin synthetizing enzymes *Ptges* and *Ptges2* after TA muscle injury (notexin) ($n = 3$ mice with two technical replicates). Control refers to the contralateral uninjured leg. (*E*) PGE2 levels of conditioned medium from isolated fibers in the presence or absence of indomethacin (Indo) assayed by ELISA ($n = 3$ mice per condition). (*F*) MuSC numbers after 24 h treatment with vehicle or PGE2 (10 ng/mL) and subsequent culture on hydrogel until day 7 ($n = 12$ mice in four independent experiments). (*G*) Trajectories of a MuSC clone treated with vehicle (*Top*) or PGE2 (*Bottom*) by time-lapse microscopy for 38 h. (*H*) Change in MuSC cell counts (numbers) in clones tracked by time-lapse microscopy after vehicle (*Left*, $n = 40$ clones) and PGE2 treatment (*Right*, $n = 44$ clones). (*I*) Plot of time to division after plating for each MuSC clone treated with vehicle or PGE2. Clones showing a 38-h time to division refers to clones that never divided during the recorded time-lapse. The lines represent the nonlinear regression curve from Gaussian lognormal fit with $R^2 = 0.9$ (control) and 0.97 (PGE2). (*J*) Violin plot of time to division after plating in MuSC clones treated with vehicle or PGE2. (*K*) Cell sizes of tracked MuSCs treated with vehicle or PGE2. $^{**}P < 0.001$, $^{***}P < 0.0005$ $^{****}P < 0.0001$. Mann–Whitney test (*E*, *J*, and *K*); ANOVA test with Bonferroni correction for multiple comparisons (*A*, *B*, and *D*); paired *t* test (*F*). Means + SEM.

PGE2, a potent lipid mediator during acute inflammation (11), on isolated MuSCs obtained by dissociating muscle tissue followed by fluorescence activated cell sorting (FACS) (Fig. 1*A*). In accordance with receptor expression, we detected a surge in the levels of PGE2 in mouse muscle lysates 3 d after injury by standard paradigms entailing notexin injection or cryoinjury (Fig. 1 *B* and *C* and Fig. S1*A*). The concomitant transient up-regulation of its synthesizing enzymes *Ptges* and *Ptges2* was also detected (Fig. 1*D*). Although other cell types within muscles may also produce PGE2 in response to injury such as endothelial cells, inflammatory cells, and fibroadipogenic progenitors (FAPs), the myofibers that circumscribe MuSCs are a source of PGE2, as observed in conditioned medium from dissociated myofibers (Fig. 1*E*). Moreover, upon treatment of myofibers with indomethacin, a NSAID that inhibits COX-2, PGE2 synthesis is markedly reduced (Fig. 1*E*). The peak in PGE2 levels coincides temporally with the expansion of MuSCs and the well-documented accumulation of inflammatory cytokines such as TGFβ1, CCL2, IL-10, IL-1β, and TNFα after injury, where MuSC activation and expansion take place (3, 5, 7, 8). Although PGE2 has previously been implicated in the inflammatory damage response, the cellular and molecular mechanism by which it acts in muscle regeneration has yet to be resolved.

To determine whether PGE2 has a direct effect on MuSC expansion, we assessed the proliferation potential of FACS isolated MuSCs (24) treated with PGE2 (10 ng/mL) in culture. This concentration of PGE2 was selected based on a dose–response assay, which resolved the lowest drug concentration that promotes a robust MuSC proliferation response (Fig. S1*B*). We found that a 1-d exposure to PGE2 in culture induced a sixfold increase in the number of MuSCs relative to controls 1 wk later (Fig. 1*F*). This increase in cell division after PGE2 treatment was also evident by EdU incorporation (Fig. S1 *C* and *D*). Culture of MuSCs in media with charcoal-stripped serum, which is depleted of lipid components including prostaglandins (25), markedly impeded cell proliferation. Addition of PGE2 rescued this block in proliferation (Fig. S1*E*). Notably, whereas freshly isolated MuSCs expressed relatively high levels of EP4 receptor mRNA, expression progressively declined to negligible levels as the cells gave rise to increasingly differentiated muscle cells in culture. This result suggests that MuSCs are the myogenic cell type most responsive to PGE2 (Fig. 1*A*). We further analyzed the effect of PGE2 at the single cell level by tracking individual MuSCs by time-lapse microscopy analysis in a hydrogel "microwell" platform as previously described (26, 27) (Fig. 1 *G–K* and Fig. S1 *F* and *G*). Clonal assays can reveal differences that are obscured by analysis of the population as a whole. Data were collected over a 38-h time period and then analyzed using the Baxter Algorithms for Cell Tracking and Lineage Reconstruction (26–28). We observed a marked increase in cumulative cell divisions and cell numbers in response to PGE2, spanning five generations for the most robust clones (Fig. 1 *G* and *H*). The basis for the difference between PGE2-treated cells and vehicle-treated controls is that immediately following PGE2 addition after plating, entry into mitosis is accelerated, which is the cause of the subsequent increased expansion (Fig. 1 *I* and *J* and Fig. S1 *F* and *G*). The subsequent exponential increase in cells in both conditions exacerbates the difference at the onset, culminating in almost twice the number of total cells at the end of the 38-h timespan (Fig. S1*G*). The concomitant increase in the incidence of larger cell sizes observed after PGE2 treatment (Fig. 1*K*) supports its role in mitotic events (29).

PGE2 Treatment Augments Muscle Regeneration. To determine if PGE2 impacted the function of MuSCs in regeneration, we performed in vivo experiments. To monitor the dynamics of regeneration over time in a quantitative manner, we capitalized on a sensitive and quantitative BLI assay we previously developed for monitoring MuSC function after transplantation (24, 26, 27, 30). MuSCs were isolated from transgenic mice expressing both GFP and luciferase (GFP/Luc mice), and equivalent numbers of MuSCs (250 cells) were coinjected with either PGE2 or vehicle into injured *tibilais anteriors* (TAs) of NOD-SCID gamma (NSG) mice. PGE2 coinjection enhanced the regenerative capacity of MuSCs by nearly two orders of magnitude compared with controls assessed by BLI. Histological analysis reveals GFP^+ MuSC engraftment in the niche and GFP^+ fibers resulting from fusion over the time course (Fig. 2*A* and Fig. S2 *A* and *B*). Moreover, following engraftment, a secondary injury elicited a spike in BLI signals of PGE2-treated MuSCs relative to controls, suggesting enhanced stem-cell repopulation (Fig. 2*A*). Notably PGE2 is known to have a relatively short half-life in vivo (31). Thus, these experiments demonstrate that transient exposure of MuSCs to PGE2 at the time of codelivery to injured muscle suffices to significantly enhance muscle regeneration.

We postulated that delivery of PGE2 alone could increase endogenous MuSC numbers and enhance regeneration, circumventing the need for a cell therapeutic. We reasoned that PGE2 delivered during the early time window immediately after injury could augment the beneficial effects of the innate inflammatory response and PGE2 surge. To test this possibility, muscles of young mice were injured, and 2 d later, we injected a bolus of PGE2 (Fig. 2*B*). We observed a striking increase (65 ± 7%) in endogenous PAX7-expressing MuSCs in the classic satellite cell niche beneath the basal lamina and atop myofibers 14 d after injury (Fig. 2 *B* and *C*). A striking shift in the distribution of myofibers from smaller toward larger sizes, assessed as cross-sectional area (CSA), was evident over the time course of regeneration (Fig. 2 *D* and *E* and Fig. S2 *C* and *D*). This change reflects the remodeling of myofiber architecture that accompanies the observed accelerated regeneration, as muscle mass did not increase during this time period (Fig. S2*E*). In addition, we tracked the response to injury and PGE2 of endogenous MuSCs by luciferase expression using a transgenic mouse model, $Pax7^{CreERT2}$;*Rosa26-LSL-Luc* (Fig. 2 *F* and *G*). The BLI data were in agreement with the histological data (Fig. 2 *B* and *C*). That a single injection of PGE2 after injury could suffice to boost endogenous MuSC numbers and regenerative function leading to this degree of accelerated regeneration was quite unexpected.

EP4 Receptor Mediates PGE2 Signaling to Promote MuSC Proliferation and Engraftment. PGE2 is known to signal through four G protein-coupled receptors (*Ptger*1–4; EP1-4) (6, 11), but the expression of these receptors in MuSCs has not previously been reported. An analysis of the transcript levels of the different receptors (*Ptger*1–4) revealed that 24 h after PGE2 treatment, the most highly expressed receptor in MuSCs is *Ptger4* (Fig. 3*A*). PGE2-treated MuSCs showed elevated downstream intracellular cAMP levels (Fig. 3*B*), a response associated with EP4 signaling (11), and in the presence of an EP4 antagonist, ONO-AE3-208, the increased proliferation response induced by PGE2 was blunted (Fig. 3*C*). These data confirm that PGE2 signals through the EP4 receptor to promote proliferation. The specificity of PGE2 for EP4 was most clearly shown by the marked reduction in proliferation of MuSCs lacking the receptor following Cre-mediated conditional ablation of EP4 in MuSCs isolated from $EP4^{f/f}$ mice (Fig. 3*D* and Fig. S3 *A–D*). A requirement for EP4 in MuSC proliferation was confirmed by tamoxifen treatment of MuSCs isolated from $Pax7^{CreERT2}$:$EP4^{f/f}$ mice in which Cre-mediated EP4 ablation is under the control of the MuSC-specific Pax7 promoter (Fig. S3 *E* and *F*). Notably, compensation by other PGE2 receptors does not occur in MuSCs lacking EP4 as expression of EP1, EP2, and EP3 receptors (*Ptger1–3*) remains low in MuSCs (Fig. S3*G*). Together, these data show that PGE2 and its receptor EP4 are crucial for MuSC proliferation. To determine if EP4 plays a role in MuSC function in vivo, we transplanted luciferase-expressing MuSCs that lacked the EP4 receptor following conditional ablation in culture into injured TAs of NSG mice. The BLI signal that was initially detected progressively declined to levels below the threshold of significance (Fig. 3*E* and Fig. S3 *A–D*). Thus, in the absence of PGE2 signaling via the EP4 receptor, regeneration is impaired.

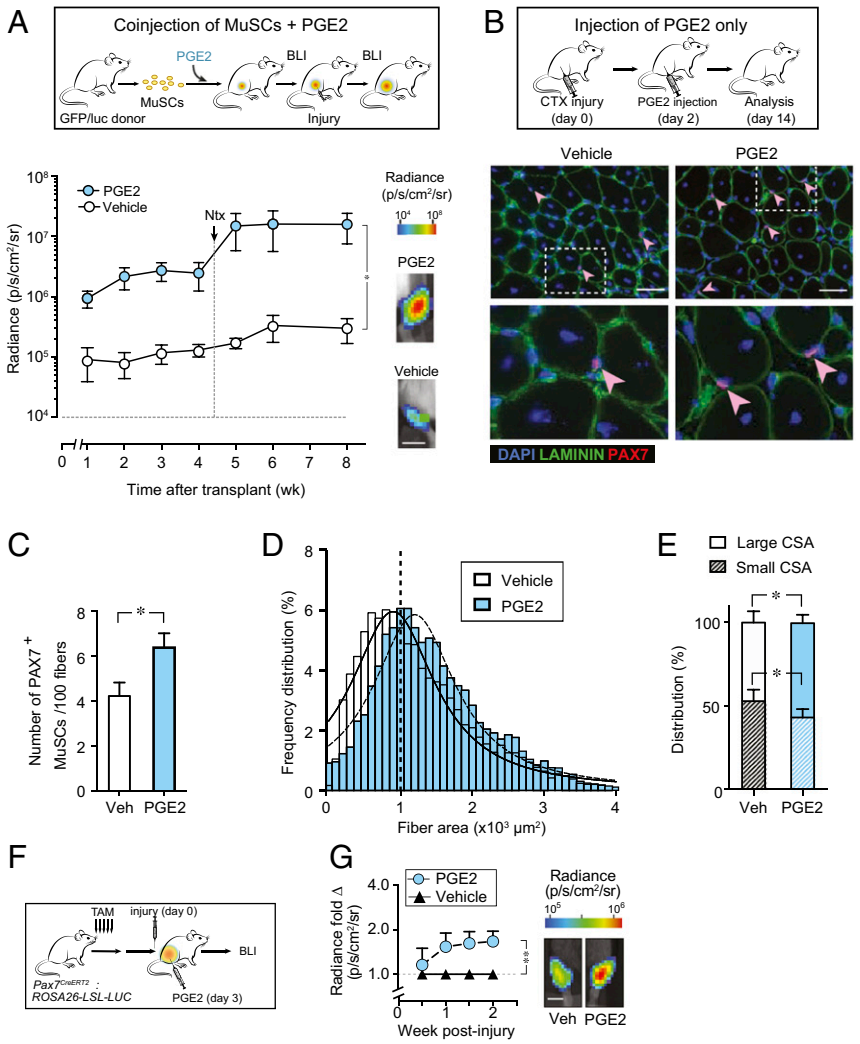

Fig. 2. PGE2 treatment augments muscle regeneration. (*A*) Engraftment of freshly sorted GFP/luc-labeled MuSCs (250 cells) coinjected with vehicle or PGE2. (*Top*) Transplant scheme. (*Bottom*) BLI signals after transplant expressed as average radiance (p·s^{-1}·cm^{-2}·sr^{-1}) (n = 4 and n = 5 mice for vehicle and PGE2-treated, respectively). At 4 wk after transplant, recipient mice were reinjured with Notexin. (*B–E*) TAs of mice were injected with vehicle or PGE2 after cardiotoxin (CTX) injury (n = 3 mice per condition, vehicle-treated is the contralateral leg). (*B*, *Top*) Experimental scheme. (*Bottom*) Representative TA cross-section. DAPI, blue; LAMININ, green; PAX7, red. Arrowheads indicate PAX7$^+$ MuSCs. (Scale bar, 40 µm.) (*C*) Quantification of PAX7$^+$ satellite cells per 100 fibers. (*D*) Representative myofiber CSAs in vehicle (open white bar) and PGE2-treated (filled blue bar) TAs. (*E*) Distribution of small (<1,000 µm^2 CSA) and large (>1,000 µm^2 CSA) myofibers. (*F* and *G*) Endogenous MuSCs assayed in *Pax7^{CreERT2};Rosa26-LSL-Luc* mice treated with tamoxifen (TAM) by BLI (n = 3 mice per condition). (*F*) Experimental scheme. (*G*, *Left*) BLI (n = 3 mice per condition). (*Right*) Representative BLI image. (Scale bar, 5 mm.) *P < 0.05. ANOVA test for group comparisons and significant difference for endpoint by Fisher's test (*A* and *G*) and paired t test (*C* and *E*). Means + SEM.

Transcription Factor *Nurr1* Is a Downstream Mediator of PGE2/EP4 Signaling in MuSCs. To perform an unbiased search for mediators of signaling downstream of PGE2 that mediate the enhanced effect of MuSC functions, we performed an RNA-sequencing (RNA-seq) analysis comparing isolated MuSCs treated with vehicle (control) or PGE2 for 24 h (Fig. S4*A*). Bioinformatics analyses using Ingenuity Pathway Analysis (IPA) and Metacore software packages revealed that in addition to regulators of PGE2 metabolism, PGE2 treatment of MuSCs led to an increase in molecular and cellular functions consistent with stem-cell expansion, including cAMP signaling, and cell-cycle regulation (Fig. S4 *B* and *C*). Among the top 200 differentially expressed genes with a nonadjusted P value < 0.05, only 11 transcription factors were identified (Fig. 4*A*). *Nurr1* was among the few that were differentially expressed. *Nurr1* had also previously been shown to mediate PGE2 signaling through cAMP and phospho-CREB to induce cell proliferation in colorectal cancer and neuronal cells (32, 33). To investigate its putative role as a downstream effector of EP4 signaling in MuSCs, we examined its expression in vivo. Remarkably, the time window of *Nurr1* expression mirrored that of PGE2 in muscle tissue, peaking at day 3 after injury (Figs. 1*B* and 4*B*). In culture, PGE2 treatment increased *Nurr1* mRNA and protein expression (Fig. 4 *C* and *D*), and *Nurr1* knockdown blunted the effect of PGE2 in inducing MuSC proliferation (Fig. 4*E* and Fig. S4*D*). To determine the specificity of *Nurr1* transcriptional regulation to PGE2-mediated EP4 receptor signaling, we ablated the EP4 receptor in *Pax7^{CreERT2}:EP4$^{f/f}$* MuSCs by tamoxifen treatment (Fig. S4*E*). *Nurr1* was not up-regulated after PGE2 treatment in EP4 knockout MuSCs (Fig. 4*F*). Expression of *Nurr1* was highest in MuSCs and declined at the onset of differentiation of myogenic cells, in accordance with the expression pattern of EP4 (Fig. 4*G*). Together, these data implicate the transcription factor NURR1 as a mediator of PGE2/EP4 signaling that triggers MuSC expansion.

Loss of PGE2 Signaling Impairs Muscle Regeneration and Strength. To determine if EP4 is required for regeneration in vivo, we used the *Pax7^{CreERT2}:EP4$^{f/f}$* mouse model in which EP4 is specifically and

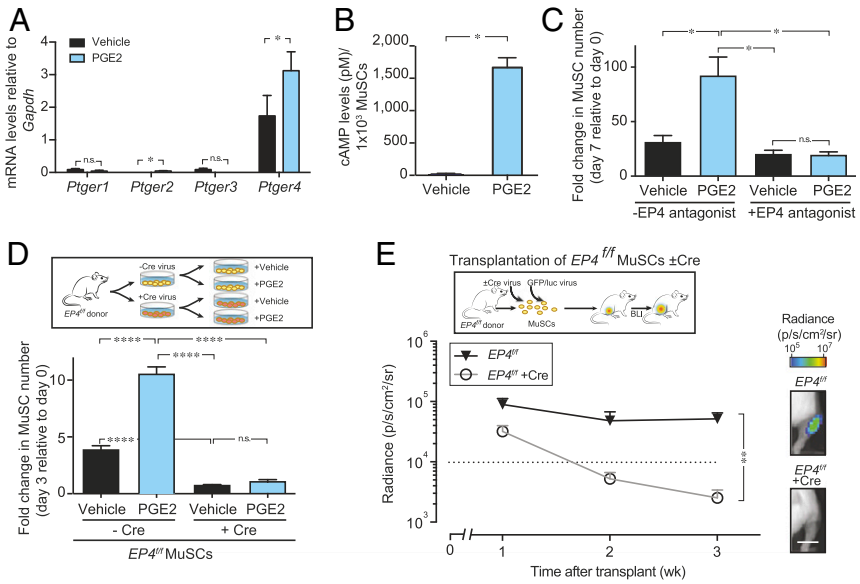

Fig. 3. EP4 mediates PGE2 signaling in MuSCs. (*A*) Expression of prostaglandin receptors (*Ptger 1–4*) by MuSCs after 24-h treatment with vehicle or PGE2 ($n = 3$ mice with two technical replicates). (*B*) cAMP levels in MuSCs after 1-h PGE2 treatment ($n = 6$ mice with three technical replicates assayed in 2 independent experiments). (*C*) MuSC numbers after 24-h treatment with vehicle or PGE2 in the absence or presence of EP4 antagonist (ONO-AE3-208, 1 μM). (*D*) Proliferation of EP4-null MuSCs treated with vehicle or PGE2. $EP4^{f/f}$ MuSCs were treated with lentiviral vector encoding Cre (+Cre, EP4-null) or without (–Cre; control) to delete *EP4* alelles. (*Top*) Scheme depicting EP4-null and control MuSC analysis. (*Bottom*) EP4-null and control MuSC numbers ($n = 6$ mice in two independent experiments). (*E*) Engraftment of GFP/luc-labeled $EP4^{f/f}$ MuSCs (1,000 cells) treated with Cre (+Cre) or without (–Cre; empty vector) in culture to delete *EP4* alelles. $EP4^{f/f}$ MuSCs were transduced with a lentiviral vector encoding GFP/luciferase for BLI. (*Top*) Transplant scheme. (*Bottom Left*) BLI signals after transplant ($n = 5$ mice per condition). (*Bottom Right*) Representative BLI image. (Scale bar, 5 mm.) $^*P < 0.05$, $^{**}P < 0.001$, $^{****}P < 0.0001$. (*A* and *B*) Mann–Whitney test; (*C* and *D*) ANOVA test with Bonferroni correction for multiple comparisons; (*E*) ANOVA test for group comparisons and significant difference for endpoint by Fisher's test. Means + SEM. n.s., nonsignificant.

conditionally ablated in MuSCs by sequential i.p. tamoxifen injection into mice (Fig. 5*A*). Induction of EP4 ablation was highly efficient in $Pax7^+$ cells in vivo following tamoxifen treatment and injury. *Ptger4* mRNA levels detected in sorted MuSCs were 96% lower than in the control (Fig. 5 *A* and *B*). In the absence of EP4 signaling in MuSCs, we observed an aberrant persistence of immature centrally nucleated regenerating myofibers that express embryonic myosin heavy chain (eMyHC) at day 7 after injury (Fig. 5 *C* and *E*). This evidence of impaired regeneration was corroborated by a shift toward myofibers with diminished myofiber CSA relative to controls at day 21 after injury (Fig. 5 *D* and *E*). In these experiments, PGE2 can act on other cell types in muscle tissue in the course of regeneration, such as mature myofibers, FAPs, and immune cells; however, these cells were not sufficient to restore the EP4-deficient MuSC functions. These features provide strong evidence that in the absence of EP4 signaling, efficacious muscle regeneration is impeded.

We further tested whether the defects in muscle repair stemming from specific loss of EP4 in MuSCs impacted muscle strength. Strikingly, eliminating signaling through EP4 on MuSCs alone led to a 35 ± 6% and 31 ± 4% decrease in twitch and tetanus force, respectively (Fig. 5 *F*–*H*), without apparent loss of muscle mass (Fig. S5*A*). To determine if the absence of PGE2 altered muscle regeneration and strength after injury, we subjected mice to treatment with a NSAID (indomethacin). A single indomethacin injection into tibialis anterior (TA) muscles of a $Pax7^{CreERT2}$; *Rosa26-LSL-Luc* mouse model 3 d after injury led to a decline in BLI relative to controls, indicative of an impairment in MuSC expansion and regeneration (Fig. 5 *I* and *J*). This loss of regenerative capacity after NSAID treatment was accompanied by a substantial 33 ± 7% reduction in twitch force compared with controls (Fig. 5 *K* and *L* and Fig. S5*B*). The diminished strength seen upon global muscle inhibition of PGE2 synthesis mirrored that observed in regenerating muscle with MuSC-EP4–specific knockout, suggesting that MuSC expansion accounts for the majority of the PGE2-mediated effects on muscle regeneration.

Discussion

We have discovered that a major effect of PGE2 is to induce muscle stem-cell expansion during muscle regeneration. PGE2 has been implicated as an immunomodulator that acts on neutrophils, mast cells, and macrophages that are crucial to the early inflammatory response after injury. The ensuing cytokine storm is thought to induce MuSC function in regeneration (3, 6, 7, 11). Studies in whole-body COX-2 KO mice, in which all prostaglandin synthesis was ablated, supported this conclusion (15, 19). Myoblasts have been proposed as the cell type responsive to PGE2 in culture (14, 16–18, 34, 35), but these cells perform poorly in regeneration (24) and cannot account for the observed effects. Moreover, other studies implicating PGE2 in regeneration all suffered from pleiotropic effects on a multiplicity of cell types.

MuSCs are crucial to development and regeneration (1–3, 24, 36–38), and their numbers dramatically increase in response to insults that damage the muscles in mice and humans (5, 20, 39–42). Injections of MuSCs into injured muscles lead to their exponential increase, whereas injection of their myoblast derivatives results in a decline in numbers, revealing a remarkable distinction in regenerative capacity of these two cell types (24). Here we show that the major effect of PGE2 during muscle regeneration is on MuSCs and that this effect is direct and mediated by the EP4 receptor. Notably, EP4 is robustly expressed on MuSCs and progressively diminishes to negligible levels on differentiating myoblasts, suggesting that the most responsive myogenic cell type to PGE2 is the MuSC. Mechanistically, once PGE2 engages the EP4 receptor, it activates cAMP and the downstream proliferation-inducing transcription factor *Nurr1*, leading to accelerated MuSC proliferation (Fig. 6). Although Nurr1 has been associated in intestinal epithelial cells with induction of proliferation and regeneration by directly blocking the

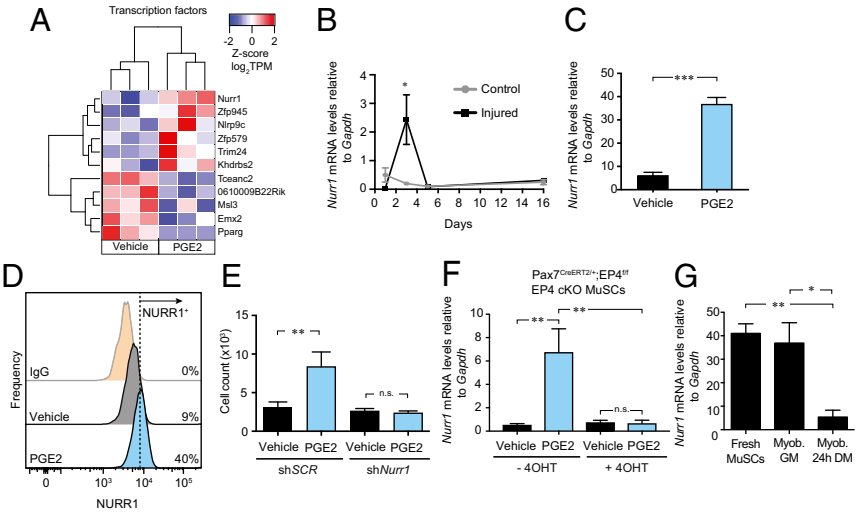

Fig. 4. *Nurr1* is a downstream effector of PGE2/EP4 signaling in MuSCs. (*A*) Heat map of differentially expressed transcription factors in vehicle or PGE2-treated MuSCs after 24 h. (*B*) Expression of *Nurr1* after TA muscle injury (notexin) ($n = 3$ mice per timepoint). (*C*) Expression of *Nurr1* by MuSCs after 24-h treatment with vehicle or PGE2 ($n = 3$ mice, performed in three independent experiments). (*D*) Flow cytometric analysis of NURR1 or IgG control in myogenic progenitors treated with vehicle or PGE2 for 24 h. (*E*) MuSC numbers after 24-h treatment of PGE2 or vehicle and subsequent culture on hydrogel until day 7 of shSCR or sh*Nurr1*-transfected cells ($n = 6$ mice, performed in two independent experiments). (*F*) Expression of *Nurr1* in *Pax7^{CreERT2}:EP4$^{f/f}$* (EP4 cKO) MuSCs treated with or without 4-hydroxytamoxifen (4OHT) in vitro and subsequently exposed to vehicle or PGE2 for 24 h ($n = 3$ mice). (*G*) Expression of *Nurr1* in MuSCs, primary myoblasts cultured in growth medium (Myob. GM), and differentiating primary myoblasts cultured in differentiation medium for 24 h (Myob. DM) ($n = 3$ biological replicates per condition). $*P < 0.05$, $**P < 0.001$, $***P < 0.0005$. ANOVA test with Bonferroni correction for multiple comparisons (*B* and *E*–*G*) and Mann–Whitney test (*C*). Means + SEM. n.s., nonsignificant.

cell cycle inhibitor p21 (Waf1/Cip1) in intestinal epithelial cells (43), its role in the expansion of stem cells, and particularly MuSCs, has not previously been described. The finding that further substantiates that *Nurr1* mediates the onset of MuSC proliferation in vivo is that its levels transiently peak in muscle tissues 3 d after injury, concomitant with the observed surge in PGE2.

We show that MuSC function and engraftment are strictly dependent on PGE2 signaling through its receptor by its conditional and specific ablation of EP4 using two approaches. Ablation of EP4 on MuSCs in vitro followed by transplantation in vivo leads to diminished engraftment evident by BLI. The most striking evidence of a crucial role for EP4 derives from its in vivo ablation of EP4 specifically on endogenous MuSCs, which causes a marked reduction in muscle strength after injury accompanied by a shift toward smaller and more immature myofibers relative to controls (Fig. 6). Thus, in the absence of the EP4 receptor, regeneration by both transplanted and endogenous MuSCs is severely impaired.

The surge in PGE2 after injury is transient. Similarly, acute PGE2 treatment enhances and accelerates muscle regeneration long-term. When freshly isolated MuSCs were coinjected with PGE2 into injured muscles, a boost in muscle repair was evident by BLI. A single ex vivo exposure of hematopoietic stem cells to PGE2 had a similarly pronounced effect on subsequent stem cell expansion and reconstitution of the blood after transplant (44). Indeed, a single injection of PGE2 alone (without MuSCs) directly into injured muscles led to a striking increase in endogenous MuSC numbers and myofiber sizes that was apparent within 2 wk. The beneficial effects of delivery of the inhibitor of the PGE2-degrading enzyme (15-PGDH) SW033291 on hematopoietic, liver, and colon regeneration are likely due to a similar augmentation of endogenous PGE2 levels (45). Notably, PGE2 and its analogs have safely been used in patients for more than a decade, for instance to induce labor (46) and to promote hematopoietic stem-cell transplantation (44). Together with our findings, these studies pave the way for its clinical use in boosting muscle repair after injury.

We show that PGE2 levels act as a rheostat that controls the efficacy of regeneration. Augmentation of the inflammatory PGE2 response to injury leads to accelerated MuSC expansion and muscle regeneration. By contrast, NSAID administration at the time of injury to control pain, a common practice, abrogates that effect, suggesting that PGE2 signaling during this early temporal window is crucial to its beneficial effects. Most striking is our finding that a single PGE2 treatment suffices to rapidly and robustly invoke a MuSC response to enhance regeneration of damaged muscle and restore strength.

Materials and Methods

Mice. We performed all experiments and protocols in compliance with the institutional guidelines of Stanford University Institutional review board (IRB) and Administrative Panel on Laboratory Animal Care (APLAC). We obtained young wild-type C57BL/6 mice from Jackson Laboratory. Double-transgenic GFP/luc mice were obtained as described previously (Jackson Laboratory, Stock 008450) (24). NSG were obtained from Jackson Laboratory (Stock 0055570). EP4$^{flox/flox}$ (EP4$^{f/f}$) mice were a kind gift from K. Andreasson, Department of Neurology & Neurological Sciences, Stanford University School of Medicine, Stanford, CA (Jackson Laboratories, Stock 028102) (47). Double-transgenic Pax7^{CreERT2};EP4$^{f/f}$ were generated by crossing Pax7^{CreERT2} mice obtained from Jackson Laboratory (Stock 017763) (48) and EP4$^{f/f}$ mice. Double-transgenic Pax7^{CreERT2};Rosa26-LSL-Luc were generated by crossing Pax7^{CreERT2} mice and Rosa26-LSL-Luc obtained from Jackson Laboratory (Stock 005125) (49). We validated these genotypes by appropriate PCR-based strategies. All mice from transgenic and wild-type strains were of young age (2–4 mo). All experiments were conducted using age- and gender-matched controls and littermates randomly assigned to experimental groups.

For muscle injury, notexin (10 $\mu g \cdot mL^{-1}$; Latoxan, catalog no. L8104) or cardiotoxin (10 μM; Latoxan, catalog no. L8102) injection or crioinjury was performed into the TA muscle. Details are provided in *SI Materials and Methods*.

FACS for Mouse MuSCs. We isolated and enriched MuSCs as previously described (24, 26, 27). Details are provided in *SI Materials and Methods*.

Flow Cytometric Analysis. We analyzed NURR1 levels by flow cytometry using myogenic progenitors after a 24-h treatment of vehicle (DMSO) or PGE2 (10 ng/mL) or from MuSCs transfected with shSCR or shNurr1 (see *Knockdown Assays*). We collected cells by incubation with 0.5% trypsin in PBS for 2 min at 37 °C. We fixed the cells using 1.6% paraformaldehyde in PBS and then permeabilized them in ice-cold methanol. We then blocked them in staining buffer (0.5% BSA in PBS) for 30 min at room temperature and stained them with a mouse monoclonal anti-Nurr1 (Abcam, catalog no. ab41917, 1:75)

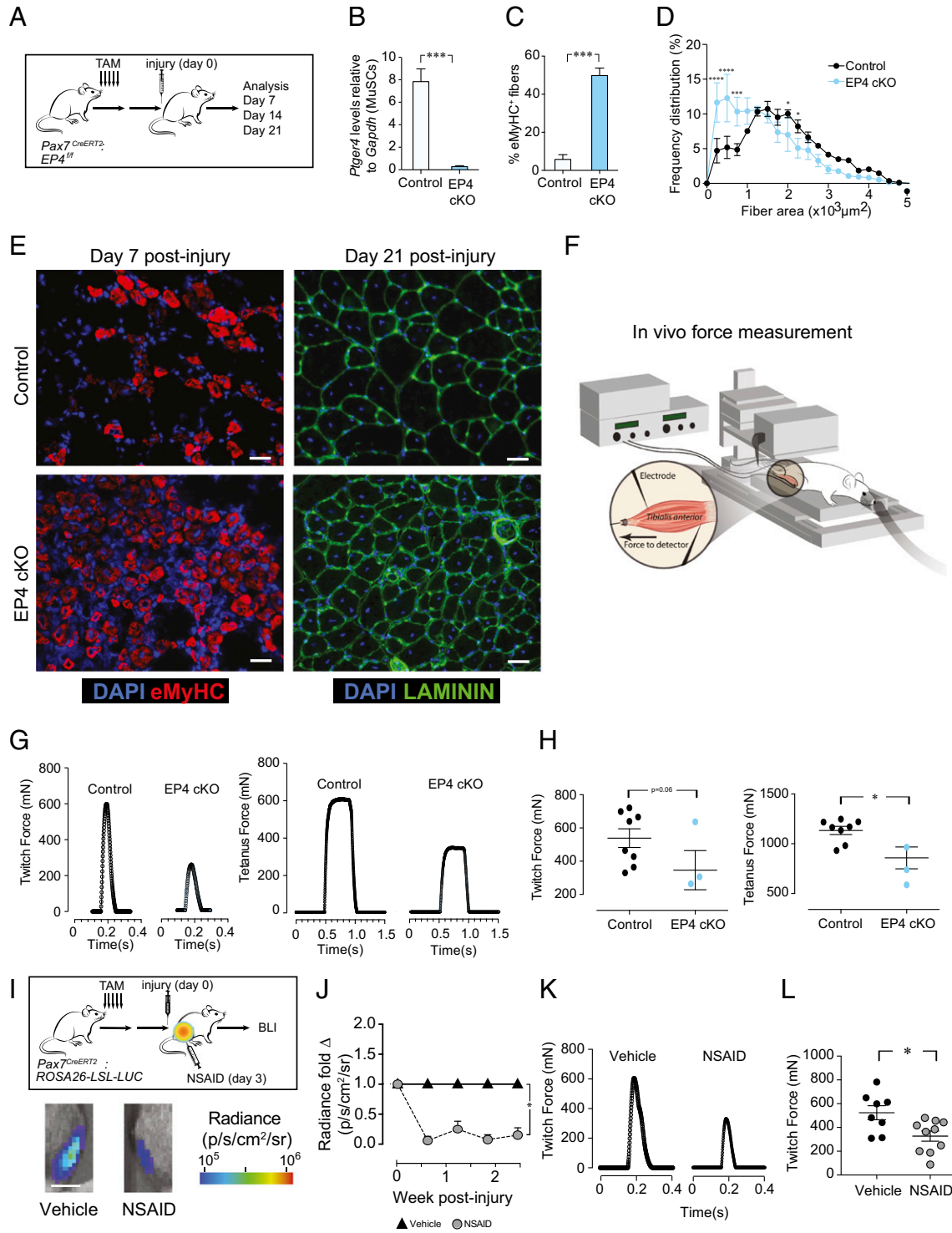

Fig. 5. Loss of function of PGE2 signaling in MuSCs impairs muscle regeneration and strength. (*A–H*) TAs of Pax7-specific EP4 conditional knockout mice (*Pax7^{CreERT2};EP4$^{f/f}$*, EP4 cKO) treated with tamoxifen (TAM) were assayed at 7 (*C* and *E*), 14 (*G* and *H*), and 21 (*B* and *D*) d after notexin injury ($n = 3$ mice per condition for all timepoints). (*A*) Experimental scheme. (*B*) Expression of *Ptger4* (EP4 receptor) in sorted MuSCs (α^{7+} CD34^{+} lin^{-}) from control or EP4 cKO mice 21 d after injury. (*C*) Percentage of eMyHC-positive fibers 7 d after injury. (*D*) Myofiber CSAs in control and EP4 cKO TAs 21 d after injury. (*E*) Representative TA cross-section at 7 d after injury—DAPI, blue; eMyHC, red (*Left*); and at 21 d after injury—DAPI, blue; LAMININ, green (*Right*). (Scale bar, 40 µm.) (*F*) In vivo muscle contractile force assay scheme. (*G*) Representative twitch force (*Left*) and tetanic force (*Right*) at 14 d after notexin injury. (*H*) Quantification of muscle twitch forces (*Left*) and tetanic forces (*Right*) ($n = 8$ for control and 3 for EP4 cKO). (*I* and *J*) Endogenous MuSCs assayed in *Pax7^{CreERT2};Rosa26-LSL-Luc* mice treated with tamoxifen (TAM) by noninvasive BLI after injection with vehicle or NSAID (Indomethacin) after cardiotoxin injury into the TA. (*I*) Experimental scheme (*Top*). Representative BLI image (*Bottom*). (Scale bar, 5mm.) (*J*) BLI ($n = 3$ mice per condition performed in two independent experiments; figure is representative of one experiment). (*K* and *L*) Muscle force was measured after vehicle or NSAID (Indomethacin) at day 14 after cardiotoxin in C57BL/6 mice (2–4 mo old). (*K*) Representative twitch force. (*L*) Quantification of muscle twitch forces ($n = 8$ for vehicle-treated and 10 for NSAID-treated). $^{*}P < 0.05$, $^{***}P < 0.0005$, $^{****}P < 0.0001$. Mann–Whitney test (*B*, *C*, *H*, and *L*); ANOVA test for group comparison and significant difference for each bin by Fisher's test (*D*); ANOVA test for group comparisons and significant difference for endpoint by Fisher's test (*J*). Means + SEM.

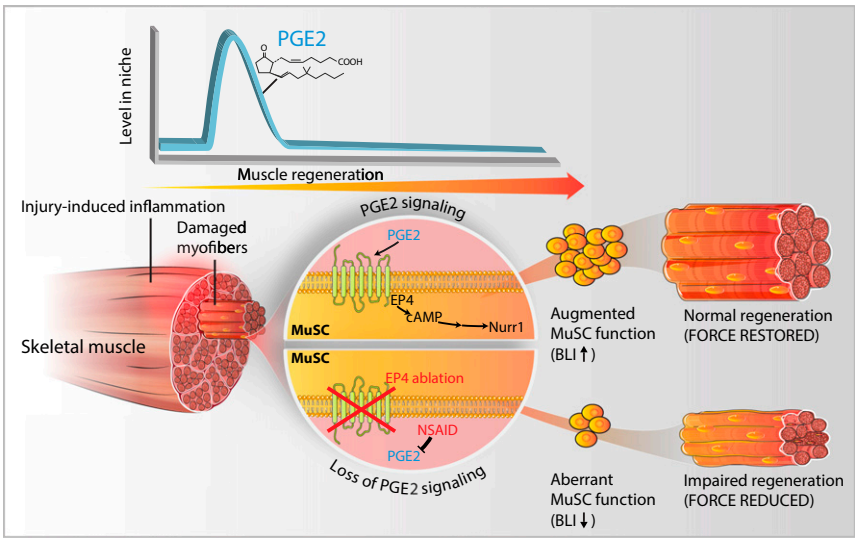

Fig. 6. Model for PGE2 signaling to expand MuSC function in regeneration. Schematic of the role of PGE2 in MuSCs. After injury, PGE2 released into the muscle niche acts on the EP4 receptor, which signals through cAMP/phospho-CREB leading to the expression of *Nurr1* proliferation-inducing transcription factor. This promotes MuSC expansion for efficient muscle regeneration. Loss of PGE2/EP4 signaling by NSAID treatment or specific loss of EP4 receptor leads to aberrant MuSC function and impaired muscle regeneration and strength recovery.

primary antibody or anti-mouse IgG control (Jackson ImmunoResearch Laboratories). Then, we stained cells with Pacific Blue-conjugated goat anti-mouse secondary antibody (Thermo Fisher Scientific, catalog no. P-10994, 1:500). We analyzed the cells on a FACS LSR II cytometer using FACSDiva software (BD Biosciences) in the Stanford Shared FACS Facility, purchased using NIH S10 Shared Instrument Grant S10RR027431-01.

MuSC Transplantation. We transplanted 250 freshly isolated MuSCs (Fig. 2*A*) or 1,000 cultured MuSCs (Fig. 3*E*) into the TA muscles of recipient mice as previously described (24, 26, 27). Details are provided in *SI Materials and Methods*.

BLI. We performed BLI using a Xenogen-100 system, as previously described (24, 26, 27, 30). Details are provided in *SI Materials and Methods*.

Hydrogel Fabrication. We fabricated polyethylene glycol (PEG) hydrogels from PEG precursors, synthesized as described previously (27). Details are provided in *SI Materials and Methods*.

MuSC Culture, Treatment, and Lentiviral Infection. Following isolation, we resuspended MuSCs in myogenic cell culture medium containing DMEM/F10 (50:50), 20% FBS, 2.5 ng·mL^{-1} fibroblast growth factor-2 (FGF-2 also known as bFGF) and 1% penicillin–streptomycin. We seeded MuSC suspensions at a density of 500 cells per cm^2 surface area. We maintained cell cultures at 37 °C in 5% CO_2 and changed medium every other day. For PGE2, EP4 receptor antagonist treatment studies, we added 1–200 ng/mL Prostaglandin E2 (Cayman Chemical) (unless specified in the figure legends, 10 ng/mL was the standard concentration used), and/or 1 μM EP4 antagonist (ONO-AE3-208, Cayman Chemical) to the MuSCs cultured on collagen-coated dishes for the first 24 h. The cells were then trypsinized and cells reseeded onto hydrogels for an additional 6 d of culture. All treatments were compared with their solvent (DMSO) vehicle control. For stripped serum assays, we resuspended isolated MuSCs in stripped serum medium containing DMEM/F10 (50:50), 20% charcoal stripped FBS (Gibco, cat no. 12676011), 2.5 ng·mL^{-1} bFGF, and 1% penicillin–streptomycin. For these experiments, MuSCs were cultured on hydrogels and vehicle (DMSO), or 10 ng/mL PGE2 (Cayman Chemical) was added to the cultures with every media change (every 2 d). Proliferation (see below) was assayed 7 d later. We performed all MuSC culture assays and transplantations after 1 wk of culture unless noted otherwise.

For *EP4$^{f/f}$* MuSCs studies, we isolated MuSCs as described above (*FACS for Mouse MuSCs*) and infected all cells with lentivirus encoding EF1α-luc-IRES-GFP (GFP/luc virus) for 24 h in culture as described previously (26), and a subset of them was coinfected with a lentivirus encoding pLM-CMV-R-Cre (mCherry/Cre virus) for 24 h in culture. pLM-CMV-R-Cre was a gift from Michel Sadelain, Memorial Sloan-Kettering Cancer Center, New York (Addgene plasmid 27546) (50). We transplanted *EP4$^{f/f}$* MuSCs (1,000 cells) into young (2–4 mo) 18-gy irradiated TAs of NSG recipient mice. For in vitro proliferation assays, *EP4$^{f/f}$* MuSCs were plated on hydrogels after infection and treated for 24 h with vehicle (DMSO) or 10 ng/mL PGE2, and proliferation was assayed 3 d later. Cells were assayed for GFP and/or mCherry expression 48 h after infection using an inverted fluorescence microscope (Carl Zeiss Microimaging). Additionally, we also performed experiments with MuSCs isolated from *Pax7^{CreERT2};EP4$^{flox/flox}$* or control *Pax7$^{+/+}$;EP4$^{flox/+}$* littermates. MuSCs were plated on collagen-coated plates and treated with 1 μM 4-hydroxy tamoxifen or vehicle (95% ethanol) during 48 h and then either passed onto hydrogels to assess proliferation 7 d later or treated with PGE2 or vehicle and collected for analysis. MuSCs are freshly isolated from the mice by FACS and put in culture for a maximum time period of 1 wk; therefore, mycoplasma contamination is not assessed.

Clonal MuSC Proliferation and Fate Analyses. We assayed clonal MuSC proliferation by time-lapse microscopy as previously described (26, 27). Details are provided in *SI Materials and Methods*.

Proliferation Assays. To assay proliferation, we used three different assays (hemocytometer, VisionBlue, and EdU). Details are provided in *SI Materials and Methods*.

Knockdown Assays. For *Nurr1* silencing in MuSCs, lentiviruses containing pLKO.1-scramble shRNA (shSCR) and pLKO.1-*Nurr1* shRNA (Mission shRNA, TRCN0000026029, Sigma) were produced in 293T cells using the packaging plasmids pLP1, pLP2, and pLP/VSVG (Invitrogen) by cotransfecting all plasmids using FuGENE-6 (Promega) according to the manufacturer's protocol. Cells were plated the day before infection, and supernatants were collected every 12 h for 2 d from 293T cells. Freshly sorted MuSCs were seeded on collagen-coated plates for 24 h and were then infected with the lentiviruses. Forty-eight hours after, cells were passed onto hydrogels and treated with PGE2 or vehicle (DMSO) for 24 h. Proliferation was assayed 7 d later.

Quantitative RT-PCR. We isolated RNA from MuSCs using the RNeasy Micro Kit (Qiagen). For muscle samples, we snap-froze the tissue in liquid nitrogen, homogenized the tissues using a mortar and pestle, followed by syringe and needle trituration, and then isolated RNA using TRIzol (Invitrogen). We reverse-transcribed cDNA from total mRNA from each sample using the SensiFAST cDNA Synthesis Kit (Bioline). We subjected cDNA to RT-PCR using SYBR Green PCR Master Mix (Applied Biosystems) or TaqMan Assays (Applied Biosystems) in an ABI 7900HT Real-Time PCR System (Applied Biosystems). We amplified samples at 95 °C for 10 min and then 40 cycles at 95 °C for 15 s and 60 °C for 1 min. To quantify relative transcript levels, we used $2^{-\Delta\Delta Ct}$ to compare treated and untreated samples and expressed the results relative to *Gapdh*. For SYBR Green qRT-PCR, we used the following primer sequences:

Gapdh, forward 5′-TTCACCACCATGGAGAAGGC-3′, reverse 5′-CCCTTTTGGCTCCACCCT-3′; *Ptges,* forward 5′-GCTGTCATCACAGGCCAGA-3′, reverse 5′-CTCCACATCTGGGTCACTCC-3′; *Ptges2*, forward 5′-CTCCTACAGGAAAGTGCCCA-3′, reverse 5′-ACCAGGTAGGTCTTGAGGGC-3′; *Ptger1*, forward 5′-GTGGTGTCGTGCATCTGCT-3′, reverse 5′ CCGCTGCAGGGAGTTAGAGT-3′; and *Ptger2*, forward 5′-ACCTTCGCCATATGCTCCTT-3′, reverse 5′-GGACCGGTGGCCTAAGTATG-3′. TaqMan Assays (Applied Biosystems) were used to quantify *Pax7*, *Myogenin*, *Nurr1*, *Ptger3*, and *Ptger4* in samples according to the manufacturer instructions with the TaqMan Universal PCR Master Mix reagent kit (Applied Biosystems). Transcript levels were expressed relative to *Gapdh* levels. For SYBR Green qPCR, *Gapdh* qPCR was used to normalize input cDNA samples. For Taqman qPCR, multiplex qPCR enabled target signals (FAM) to be normalized individually by their internal *Gapdh* signals (VIC).

PGE2 ELISA. PGE2 levels were measured using a PGE2 ELISA Kit (R&D Systems, catalog no. KGE004B). Details are provided in *SI Materials and Methods*.

cAMP Activity Assay. MuSCs were treated with DMSO (vehicle) or PGE2 (10 ng/mL) for 1 h and cAMP levels measured according to the cAMP-Glo Assay protocol optimized by the manufacturer (Promega). Each sample was assayed in triplicate and in two independent experiments.

In Vivo Muscle Force Measurement. Mice were injured as described in *Muscle Injury*. Force measurements were on the TA muscles at day 14 after injury based on protocols published previously (26, 51). Details are provided in *SI Materials and Methods*.

RNA-Seq. For RNA-seq, α7-integrin^{+}CD34^{+} MuSCs were isolated as described above, seeded on collagen-coated plates, treated a day later with PGE2 or vehicle (DMSO), and processed after 24 h of treatment. RNA was isolated using Qiagen RNAEasy Micro kit from 5,000–10,000 cells and cDNA generated and amplified using NuGEN Ovation RNA-Seq System v2 kit. Libraries were constructed from cDNA with the TruSEQ RNA Library Preparation Kit v2 (Illumina) and sequenced to 30–40 $\times$ 10^6 1 $\times$ 75-bp reads per sample on a HiSEQ 2500 from the Stanford Functional Genomics Facility, purchased using NIH S10 Shared Instrument Grant S10OD018220.

RNA-Seq Analysis. For the RNA-Seq analysis, RNA sequences were aligned against the *Mus musculus* genome using STAR (52). RSEM (53) was used for calling transcripts and calculating transcripts per million (TPM) values as well as total counts. A counts matrix containing the number of counts for each gene and each sample was obtained. This matrix was analyzed by DESeq to calculate statistical analysis of significance (54) of genes between samples.

Immunofluorescence and Histology. We collected and prepared recipient TA muscle tissues for histology as previously described (26, 27). For mouse injury assays, we incubated transverse sections with Rabbit polyclonal anti-PGE2 (abcam, catalog no. ab2318, 1:100), rat polyclonal anti-Laminin (Clone A5) (EMD Millipore, catalog no. 05–206, 1:200), mouse monoclonal anti-Pax7 (Santa Cruz, catalog no. sc-81648, 1:50), AlexaFluor 647-conjugated wheat germ agglutinin (WGA) antibody (W32466, Thermo Fisher Scientific), rabbit polyclonal anti-GFP (A11122, Thermo Fisher Scientific, 1:500), and mouse monoclonal anti-eMyHC (DSHB, catalog no. F1.652, 1:10) primary antibodies and then with AlexaFluor secondary antibodies (Jackson ImmunoResearch Laboratories, 1:500). We counterstained nuclei with DAPI (Invitrogen).

Image Analysis. We acquired images with an AxioPlan2 epifluorescent microscope (Carl Zeiss Microimaging) with Plan NeoFluar 10×/0.30 N.A. or 20×/0.75 N.A. objectives (Carl Zeiss) and an ORCA-ER digital camera (Hamamatsu Photonics) controlled by the SlideBook (3i) software or with a KEYENCE BZ-X700 all-in-one fluorescence microscope (Keyence) with 20×/0.75 N.A. objectives. The images were cropped using Adobe Photoshop with consistent contrast adjustments across all images from the same experiment. The image composites were generated using Adobe Illustrator. We analyzed the number of PAX7-positive cells using the MetaMorph Image Analysis software (Molecular Devices) and the fiber area using the Baxter Algorithms for Myofiber Analysis that identified the fibers and segmented the fibers in the image to analyze the area of each fiber. For PAX7 quantification, we examined serial sections spanning a depth of at least 2 mm of the TA. For fiber area, the entire cross-section of the TA with the largest injured area was captured and stitched using the Keyence Analysis Software. Data capture and analyses were blinded. The researchers performing the imaging acquisition and scoring were unaware of treatment condition given to the sample groups analyzed.

Statistical Analysis. We performed cell culture experiments in at least three independent experiments where three biological replicates were pooled in each. In general, we performed MuSC transplant experiments in at least two independent experiments, with at least 3–5 total transplants per condition. We used a paired *t* test for experiments where control samples were from the same experiment in vitro or from contralateral limb muscles in vivo. A nonparametric Mann–Whitney test was used to determine the significance difference between vehicle-treated vs. PGE2-treated groups using $\alpha = 0.05$. ANOVA or multiple *t* test was performed for multiple comparisons with significance level determined using Bonferroni correction or Fisher's test as indicated in the figure legends. Unless otherwise described, data are shown as the mean $\pm$ SEM. Differences with P value < 0.05 were considered significant (*$P < 0.05$, **$P < 0.01$, ***$P < 0.001$, ****$P < 0.0001$).

ACKNOWLEDGMENTS. We apologize to those investigators whose important work we were unable to cite or describe owing to space constraints. We thank D. Burns for critical discussions of the manuscript; K. Koleckar for technical assistance; K. Andreasson (Department of Neurology & Neurological Sciences, Stanford University School of Medicine) for the *EP4$^{f/f}$* mice; and the Stanford Center for Innovation in In-Vivo Imaging (SCI3), the Stanford Shared FACS Facility (SSFF), FACS Core Facility in Stanford Lokey Stem Cell Research Building, the Stanford Functional Genomics Facility, and the Stanford Veterinary Service Center (VSC) for technical support. This study was supported by the Baxter Foundation, and NIH Grant AG020961 (to H.M.B.).

1. Chakkalakal JV, Jones KM, Basson MA, Brack AS (2012) The aged niche disrupts muscle stem cell quiescence. *Nature* 490:355–360.
2. Kuang S, Gillespie MA, Rudnicki MA (2008) Niche regulation of muscle satellite cell self-renewal and differentiation. *Cell Stem Cell* 2:22–31.
3. Shi X, Garry DJ (2006) Muscle stem cells in development, regeneration, and disease. *Genes Dev* 20:1692–1708.
4. Tierney MT, et al. (2014) STAT3 signaling controls satellite cell expansion and skeletal muscle repair. *Nat Med* 20:1182–1186.
5. Chazaud B (2016) Inflammation during skeletal muscle regeneration and tissue remodeling: Application to exercise-induced muscle damage management. *Immunol Cell Biol* 94:140–145.
6. Korotkova M, Lundberg IE (2014) The skeletal muscle arachidonic acid cascade in health and inflammatory disease. *Nat Rev Rheumatol* 10:295–303.
7. Tidball JG (2017) Regulation of muscle growth and regeneration by the immune system. *Nat Rev Immunol* 17:165–178.
8. Joe AW, et al. (2010) Muscle injury activates resident fibro/adipogenic progenitors that facilitate myogenesis. *Nat Cell Biol* 12:153–163.
9. Uezumi A, Fukada S, Yamamoto N, Takeda S, Tsuchida K (2010) Mesenchymal progenitors distinct from satellite cells contribute to ectopic fat cell formation in skeletal muscle. *Nat Cell Biol* 12:143–152.
10. Tidball JG (2011) Mechanisms of muscle injury, repair, and regeneration. *Compr Physiol* 1:2029–2062.
11. Ricciotti E, FitzGerald GA (2011) Prostaglandins and inflammation. *Arterioscler Thromb Vasc Biol* 31:986–1000.
12. Funk CD (2001) Prostaglandins and leukotrienes: Advances in eicosanoid biology. *Science* 294:1871–1875.
13. Simmons DL, Botting RM, Hla T (2004) Cyclooxygenase isozymes: The biology of prostaglandin synthesis and inhibition. *Pharmacol Rev* 56:387–437.
14. Beaulieu D, et al. (2012) Abnormal prostaglandin E2 production blocks myogenic differentiation in myotonic dystrophy. *Neurobiol Dis* 45:122–129.
15. Bondesen BA, Mills ST, Kegley KM, Pavlath GK (2004) The COX-2 pathway is essential during early stages of skeletal muscle regeneration. *Am J Physiol Cell Physiol* 287: C475–C483.
16. Mo C, Romero-Suarez S, Bonewald L, Johnson M, Brotto M (2012) Prostaglandin E2: From clinical applications to its potential role in bone- muscle crosstalk and myogenic differentiation. *Recent Pat Biotechnol* 6:223–229.
17. Mo C, et al. (2015) Prostaglandin E2 promotes proliferation of skeletal muscle myoblasts via EP4 receptor activation. *Cell Cycle* 14:1507–1516.
18. Otis JS, Burkholder TJ, Pavlath GK (2005) Stretch-induced myoblast proliferation is dependent on the COX2 pathway. *Exp Cell Res* 310:417–425.
19. Shen W, Prisk V, Li Y, Foster W, Huard J (2006) Inhibited skeletal muscle healing in cyclooxygenase-2 gene-deficient mice: The role of PGE2 and PGF2alpha. *J Appl Physiol* 101:1215–1221.
20. Mackey AL, et al. (2007) The influence of anti-inflammatory medication on exercise-induced myogenic precursor cell responses in humans. *J Appl Physiol* 103:425–431.
21. Schoenfeld BJ (2012) The use of nonsteroidal anti-inflammatory drugs for exercise-induced muscle damage: Implications for skeletal muscle development. *Sports Med* 42:1017–1028.
22. Lundberg I, Kratz AK, Alexanderson H, Patarroyo M (2000) Decreased expression of interleukin-1alpha, interleukin-1beta, and cell adhesion molecules in muscle tissue following corticosteroid treatment in patients with polymyositis and dermatomyositis. *Arthritis Rheum* 43:336–348.
23. Arnold L, et al. (2007) Inflammatory monocytes recruited after skeletal muscle injury switch into antiinflammatory macrophages to support myogenesis. *J Exp Med* 204: 1057–1069.

24. Sacco A, Doyonnas R, Kraft P, Vitorovic S, Blau HM (2008) Self-renewal and expansion of single transplanted muscle stem cells. *Nature* 456:502–506.
25. Smethurst M, Williams DC (1977) Levels of prostaglandin E and prostaglandin F in samples of commercial serum used for tissue culture. *Prostaglandins* 13:719–722.
26. Cosgrove BD, et al. (2014) Rejuvenation of the muscle stem cell population restores strength to injured aged muscles. *Nat Med* 20:255–264.
27. Gilbert PM, et al. (2010) Substrate elasticity regulates skeletal muscle stem cell self-renewal in culture. *Science* 329:1078–1081.
28. Magnusson KE, Jalden J, Gilbert PM, Blau HM (2015) Global linking of cell tracks using the Viterbi algorithm. *IEEE Trans Med Imaging* 34:911–929.
29. Rodgers JT, et al. (2014) mTORC1 controls the adaptive transition of quiescent stem cells from G0 to G(Alert). *Nature* 510:393–396.
30. Ho AT, Blau HM (2016) Noninvasive tracking of quiescent and activated muscle stem cell (MuSC) engraftment dynamics in vivo. *Methods Mol Biol* 1460:181–189.
31. Bygdeman M (2003) Pharmacokinetics of prostaglandins. *Best Pract Res Clin Obstet Gynaecol* 17:707–716.
32. Holla VR, Mann JR, Shi Q, DuBois RN (2006) Prostaglandin E2 regulates the nuclear receptor NR4A2 in colorectal cancer. *J Biol Chem* 281:2676–2682.
33. Volakakis N, et al. (2010) NR4A orphan nuclear receptors as mediators of CREB-dependent neuroprotection. *Proc Natl Acad Sci USA* 107:12317–12322.
34. Baracos V, Rodemann HP, Dinarello CA, Goldberg AL (1983) Stimulation of muscle protein degradation and prostaglandin E2 release by leukocytic pyrogen (interleukin-1). A mechanism for the increased degradation of muscle proteins during fever. *N Engl J Med* 308:553–558.
35. Rodemann HP, Goldberg AL (1982) Arachidonic acid, prostaglandin E2 and F2 alpha influence rates of protein turnover in skeletal and cardiac muscle. *J Biol Chem* 257: 1632–1638.
36. Mauro A (1961) Satellite cell of skeletal muscle fibers. *J Biophys Biochem Cytol* 9: 493–495.
37. Montarras D, et al. (2005) Direct isolation of satellite cells for skeletal muscle regeneration. *Science* 309:2064–2067.
38. Pawlikowski B, Pulliam C, Betta ND, Kardon G, Olwin BB (2015) Pervasive satellite cell contribution to uninjured adult muscle fibers. *Skelet Muscle* 5:42.
39. Crameri RM, et al. (2004) Changes in satellite cells in human skeletal muscle after a single bout of high intensity exercise. *J Physiol* 558:333–340.
40. Darr KC, Schultz E (1987) Exercise-induced satellite cell activation in growing and mature skeletal muscle. *J Appl Physiol* 63:1816–1821.
41. Dreyer HC, Blanco CE, Sattler FR, Schroeder ET, Wiswell RA (2006) Satellite cell numbers in young and older men 24 hours after eccentric exercise. *Muscle Nerve* 33:242–253.
42. Paulsen G, Mikkelsen UR, Raastad T, Peake JM (2012) Leucocytes, cytokines and satellite cells: What role do they play in muscle damage and regeneration following eccentric exercise? *Exerc Immunol Rev* 18:42–97.
43. Zu G, et al. (2017) Nurr1 promotes intestinal regeneration after ischemia/reperfusion injury by inhibiting the expression of p21 (Waf1/Cip1). *J Mol Med (Berl)* 95:83–95.
44. North TE, et al. (2007) Prostaglandin E2 regulates vertebrate haematopoietic stem cell homeostasis. *Nature* 447:1007–1011.
45. Zhang Y, et al. (2015) Tissue regeneration. Inhibition of the prostaglandin-degrading enzyme 15-PGDH potentiates tissue regeneration. *Science* 348:aaa2340.
46. Thomas J, Fairclough A, Kavanagh J, Kelly AJ (2014) Vaginal prostaglandin (PGE2 and PGF2a) for induction of labour at term. *Cochrane Database Syst Rev* 6:CD003101.
47. Schneider A, et al. (2004) Generation of a conditional allele of the mouse prostaglandin EP4 receptor. *Genesis* 40:7–14.
48. Murphy MM, Lawson JA, Mathew SJ, Hutcheson DA, Kardon G (2011) Satellite cells, connective tissue fibroblasts and their interactions are crucial for muscle regeneration. *Development* 138:3625–3637.
49. Safran M, et al. (2003) Mouse reporter strain for noninvasive bioluminescent imaging of cells that have undergone Cre-mediated recombination. *Mol Imaging* 2:297–302.
50. Papapetrou EP, et al. (2011) Genomic safe harbors permit high β-globin transgene expression in thalassemia induced pluripotent stem cells. *Nat Biotechnol* 29:73–78.
51. Hakim CH, Wasala NB, Duan D (2013) Evaluation of muscle function of the extensor digitorum longus muscle ex vivo and tibialis anterior muscle in situ in mice. *J Vis Exp* 72:e50183.
52. Dobin A, et al. (2013) STAR: Ultrafast universal RNA-seq aligner. *Bioinformatics* 29: 15–21.
53. Li B, Dewey CN (2011) RSEM: Accurate transcript quantification from RNA-Seq data with or without a reference genome. *BMC Bioinformatics* 12:323.
54. Anders S, Huber W (2010) Differential expression analysis for sequence count data. *Genome Biol* 11:R106.
55. Chenouard N, et al. (2014) Objective comparison of particle tracking methods. *Nat Methods* 11:281–289.
56. Maška M, et al. (2014) A benchmark for comparison of cell tracking algorithms. *Bioinformatics* 30:1609–1617.
57. Moyle LA, Zammit PS (2014) Isolation, culture and immunostaining of skeletal muscle fibres to study myogenic progression in satellite cells. *Methods Mol Biol* 1210:63–78.
58. Burkholder TJ, Fingado B, Baron S, Lieber RL (1994) Relationship between muscle fiber types and sizes and muscle architectural properties in the mouse hindlimb. *J Morphol* 221:177–190.